Tectonophysics xxx (2017) xxx–xxx

Contents lists available at ScienceDirect

Tectonophysics

journal homepage: www.elsevier.com/locate/tecto

Subducting continental lower crust and crustal thickness variations in the intermediate seismic zone of Pamir–Hindu Kush inferred from Moho underside reflection pmP

Hangqi He [a], Fa-Bin Pan [a], Hanlin Chen [b], Yujia Zhang [a], Xin Zheng [a], Xiaobo He [a,*]

[a] Department of Marine Sciences, Zhejiang University, Zhoushan, People's Republic of China
[b] School of Earth Sciences, Zhejiang University, Hangzhou, People's Republic of China

ARTICLE INFO

Article history:
Received 1 November 2016
Received in revised form 3 March 2017
Accepted 3 April 2017
Available online xxxx

Keywords:
Moho
pmP phase
Intermediate earthquake
Pamir–Hindu Kush
Lower crust

ABSTRACT

The Pamir–Hindu Kush region is an orogenic belt which formed as a result of recent continental collision between the Indian and Eurasian Plates. A comprehensive understanding of the tectonic history of this region has been hampered due to limited seismological investigations. In this study, we use the Moho underside reflection pmP phase to constrain crustal thickness variations in the intermediate-depth seismic zone (36–37°N, 69–72°E). The seismic events characterized by focal depth deeper than 100 km and magnitude > 5.8 (Mw) were used. The crustal thickness was determined by identifying the depth phase pP and the Moho underside reflection pmP. The measured thickness varies spatially from 58.1 to 76.2 km, with uncertainties most likely resulting from deviation of the average P-wave velocities (~6.21 km/s with a deviation of 0.22 km/s) in the crust. The strong Moho depth variations imply a large structural deformation of the crust, which reflects a complex collision-related mountain building history. We also detected two strong reflections from deep interfaces down to ~97 km underneath the southernmost Pamir. Based on our direct observations and waveform modeling, we interpret that the two reflections are possibly the manifestations of the underplating subducted Eurasian lower crust in this region. Our observations complement those of other seismic results, including receiver functions from previous studies.

1. Introduction

The Pamir–Hindu Kush region (Fig. 1) is one of the most tectonically active areas of continental collision in the world. It is located in the north of the western syntaxis of the India-Asia collision system, and is characterized by intermediate-depth seismicity (Bai and Zhang, 2015). This collision occurred ca. 50 Ma ago (Schwab et al., 2004; Negredo et al., 2007) when the Indian Plate subducted beneath the Eurasian Plate resulting in the closure of the Neo-Tethys Ocean (Patriat and Achache, 1984). The characteristics of the orogenic belt suggest two continental subduction zones, with the Indian Plate dipping steeply northwards underneath the Hindu Kush and southward subduction of the Eurasian Plate beneath the Pamir (Burtman and Molnar, 1993; Pegler and Das, 2002; Sippl et al., 2013a; Sobel et al., 2013; Schneider et al., 2013). This collision system is characterized by lithospheric indentation, delamination and break-off (Kufner et al., 2016). The subduction system with slab break-off below the Hindu Kush hence provides a rare glimpse on the terminal stage of subduction (Kufner et al., 2017). High-precision earthquake locations and tomographic images show that continental crustal is subducted down to 240 km and 250 km beneath the Pamir the Hindu Kush, respectively (Sippl et al., 2013a).

Tomographic inversions and receiver function analyses reveal that a substantial amount of lower crustal material was pulled down beneath the Pamir into the mantle to depths of at least 80–100 km, whereas the buoyant Eurasian upper and middle crusts avoid deep penetration into the mantle and are instead shortened and incorporated into the Pamir (Sippl et al., 2013b; Schneider et al., 2013). Regional Pn tomographic inversions reveal that the Pamir-Hindu Kush is also characterized by strong anisotropy and low velocities in the uppermost mantle (Feng and Pei, 2012). A Moho depth distribution map obtained from receiver function studies shows that crust is ~65–70 km thick at most stations in the Pamir and thickens to 70 to 75 km in the southeast, and that in the basin areas such as the Tajik basin adjacent to the Pamir a shallower Moho depth of ~40–50 km is observed (Schneider, 2014).

However, the previous seismological experiments are still limited in some aspects, especially the intermediate-depth seismic zone of the Pamir–Hindu Kush, which remains poorly investigated, with only a handful of measurements of crustal thickness conducted so far. Understanding this issue would add an essential element to the geodynamic models that decipher the Pamir–Hindu Kush subduction processes. In

* Corresponding author.
E-mail address: xbhe@zju.edu.cn (X. He).

http://dx.doi.org/10.1016/j.tecto.2017.04.004
0040-1951/

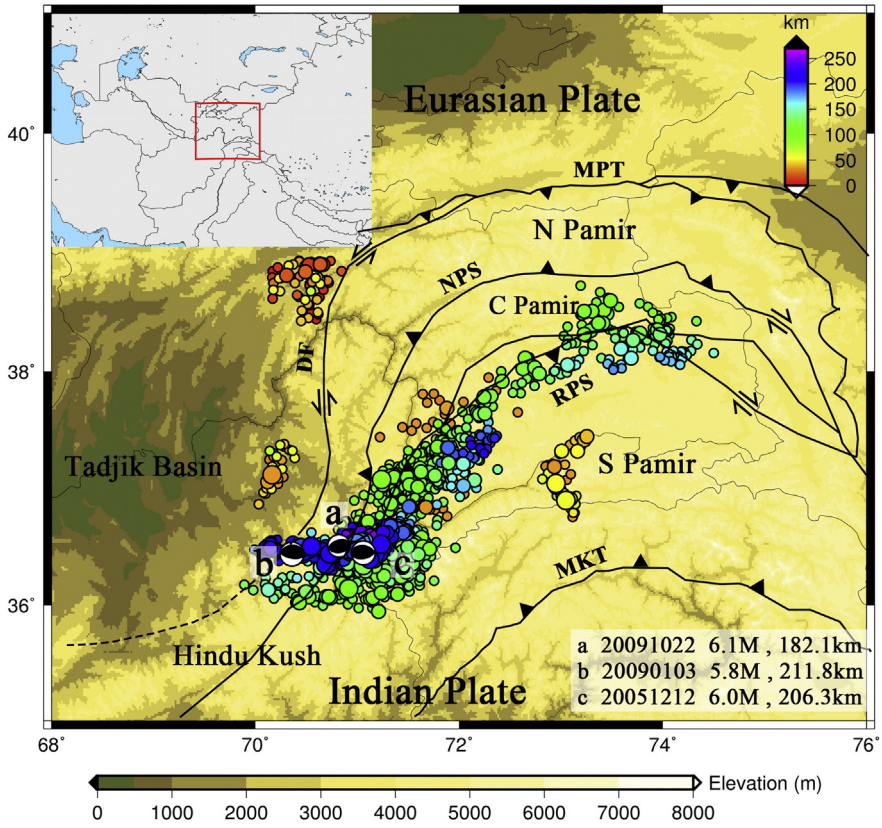

Fig. 1. A map shows the study region of the Pamir–Hindu Kush intermediate seismic zone and its surroundings. Colored circles denote historic seismicity spanning the period 1964 to 2011 with M > 4.5 (Event catalogue was taken from relocated results given by Bai and Zhang (2015)). Three beach balls depict the focal mechanism of 3 events used in this study, and events information is also detailed in the lower right corner. Faults taken from Robinson et al. (2004) and Mechie et al. (2012). DF = Darvaz Fault, MPT = Main Pamir Thrust, NPS = Northern Pamir Suture, RPS = Rushan Psart Suture, MKT = Main Karakoram Thrust. (For interpretation of the references to color in this figure legend, the reader is referred to the web version of this article.)

this study, we used the source-sided Moho underside reflection pmP phase to constrain the crustal thickness variations in the intermediate-depth seismic zone (36–37°N, 69–72°E).

2. Method

The method that was adopted in our study was pioneered by several studies (e.g., Zhang and Lay, 1993; Zandt et al., 1994) and has been successfully applied to constrain the crustal thickness beneath the Andes (e.g., McGlashan et al., 2008). The difference between the above-mentioned studies is that the former are based on S wave reflections while the latter uses P wave reflections. Compared to S waves, the frequency of P waves is higher and its arrival time can be more accurately measured; therefore, we used P waves in this study. As shown in Fig. 2a, P waves reflect from the under-side of the Moho interface and transform into pmP phase, which is sourced from intermediate to deep (sub-Moho) earthquakes. In the simulated seismic record (Fig. 2b), calculated according to a propagation matrix algorithm (Wang, 1999), the P and pP phases can be easily identified and the pmP phase arrives between them. In addition, the core-reflected PcP phase may exist;

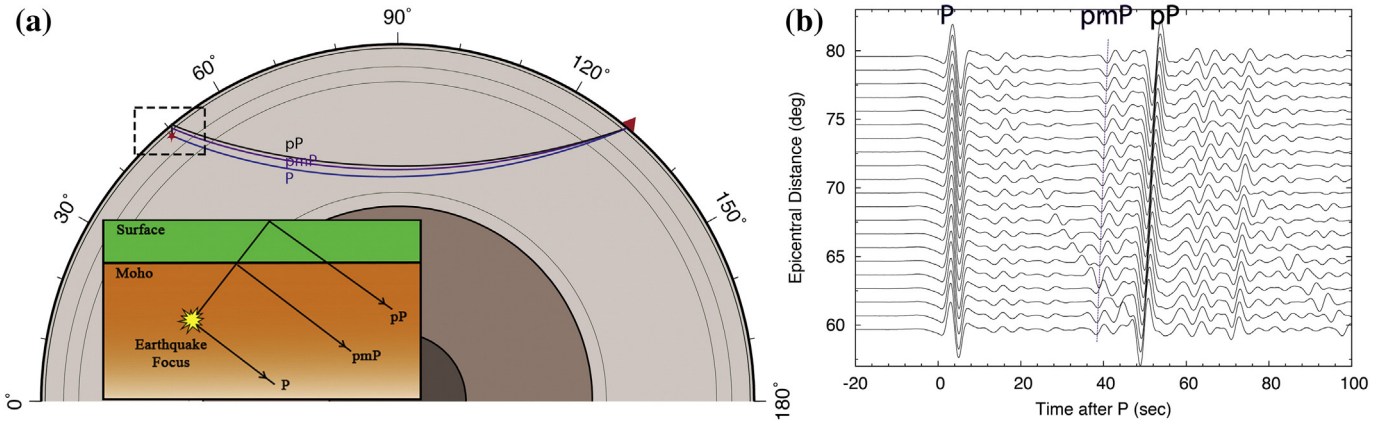

Fig. 2. (a) Illustration of P wave reflection from the underside of the Moho (pmP) and surface (pP). The inset has benefitted from McGlashan et al. (2008)'s schematic work. (b) A synthetic vertical record-section comprising P, pmP, and pP, which was calculated based on a slightly modified IASP91 model (Kennett and Engdahl, 1991).

Please cite this article as: He, H., et al., Subducting continental lower crust and crustal thickness variations in the intermediate seismic zone of Pamir–Hindu Kush inferre..., Tectonophysics (2017), http://dx.doi.org/10.1016/j.tecto.2017.04.004

however, the slowness of pmP is nearly identical to that of P and pP, which not only is of assistance in identifying the pmP signal but also facilitates enhancing the pmP signal via simple linear stacking along P or pP arrivals. The measured delay time between pmP and pP is directly related to the crustal thickness and crustal velocity by the following formula:

$$t_{pP} - t_{pmP} \approx 2h\sqrt{V_{pc}^{-2} - P^2},$$

where t_{pP} is the travel time of the pP wave, t_{pmP} is the travel time of the pmP wave, h is the crustal thickness near the source-side bounce points, V_{pc} is the velocity of the P wave in the crust, and P is the ray parameter (i.e., the horizontal slowness) for the phase. Like Zandt et al. (1994) and McGlashan et al. (2008), we assumed that the ray parameter for the pmP phase is identical to that of the pP phase, which can be calculated using the Taup toolkit (Crotwell et al., 1999) based on the IASP91 model (Kennett and Engdahl, 1991). In addition, we also assumed that the crustal thickness remains nearly constant over an area which contains all bounce points determined by the event-network distribution for each record-section. Therefore, the main task in this study was to measure the average velocity of the P wave in the crust and to calculate the time difference between pmP and pP.

The focal-depths and magnitudes of the selected events have certain requirements in this study. To ensure that Moho underside reflections occur, the focal-depths of the events selected need to be deeper than 100 km, which allows the P, pmP, and pP phases to be distinguished from each other due to sufficient time separation. A minimum magnitude of 5.8 (preferably not < 6) is necessary for the P and pP phases to have sufficient energy (McGlashan et al., 2008) so that the reflections can be readily identified on individual traces.

3. Data and analysis

3.1. Data selection and preprocessing

For this study, we downloaded seismic data from F-net and three regional networks including XS, MN, and YP from IRIS (Fig. 3). A total of three intermediate-depth events occurred in the subducted Indian Plate and were primarily distributed in the northwest part of the intermediate-depth seismic zone. A 2-pass, 2-pole Butterworth band-pass filter with corner frequencies at 0.05 Hz and 0.5 Hz were

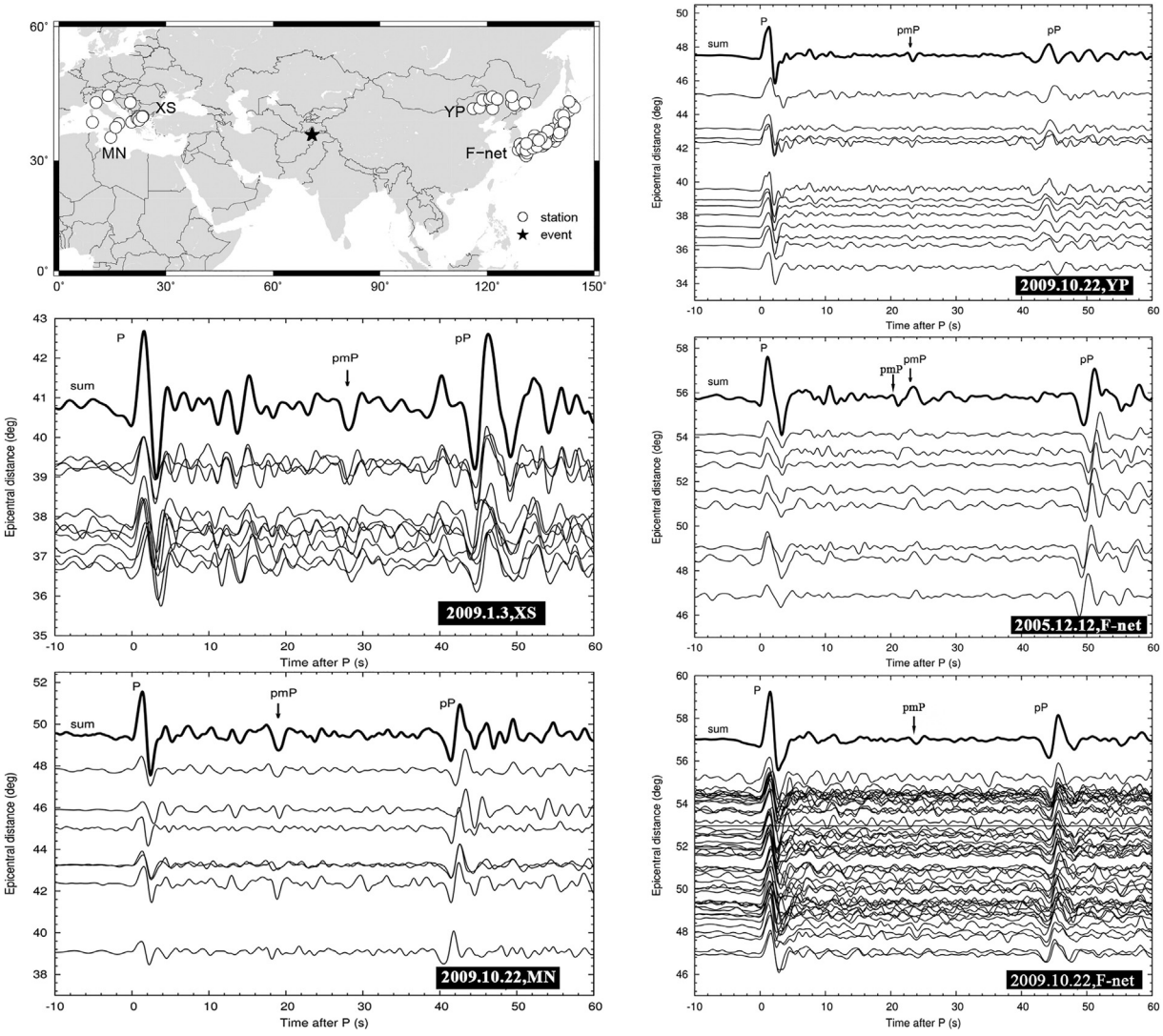

Fig. 3. The top left figure illustrates the distribution of four networks and one representative event in study area, in which a star denotes an event and open circles depict stations. The remaining plots demonstrate all the selected record-sections (vertical component) comprising clear Moho reflections (pmP) as well as surface reflections (pP). All traces filtered with a Butterworth band-pass filter were aligned along each P arrival in five profiles, and the top trace in each section corresponds to the linearly stacked waveform for the purpose of enhancing pmP. Note that there has two pmP arrivals characterized by opposite polarity shown in the section for the 2005.12.12 event recorded by F-net, which is confirmed by its vespagram (see Fig. S1 of the Supplementary material).

Please cite this article as: He, H., et al., Subducting continental lower crust and crustal thickness variations in the intermediate seismic zone of Pamir–Hindu Kush inferre..., Tectonophysics (2017), http://dx.doi.org/10.1016/j.tecto.2017.04.004

applied to the raw data. A total of five record sections were produced. We failed to obtain additional data due to the pmP phases being blurred by noise in other record-sections. The collected pmP phases are visible and can be seen even on the single traces. Note that there is one exceptional section showing two pmP arrivals characterized by opposite polarity in the 2005.12.12 event recorded by F-net; we will diagnose this observation further in the Discussion Section. To confirm the pmP observations, 4th-root slant stacking (e.g., Yang and He, 2015) was employed to calculate the vespagrams for the five record sections that clearly show signals associated with pmP waves (see Fig. S1 in the Supplementary material). Record-sections of the radial components are also presented in Fig. S2 for comparison. The radial pmP waves are less prominent compared to the vertical waves, likely due to the predominant decomposition of energy into vertical components.

Before picking the pmP phases, we stacked the waveforms from different traces generated by the same event to enhance the signal as well as to reduce the noise and the interference of other phases (such as the PcP phase). The specific process was to arrange all waveforms according to the epicentral distance, to align them by P wave, and finally to stack the waveforms. From the stacked waveform, the differential travel time between the pmP and pP waves can easily be obtained by manually picking their onsets.

Compared to the dominant signal periods of up to 2 s, the travel time differential between the closest and farthest station records was insignificant and could be reasonably ignored (McGlashan et al., 2008). Therefore, it is important to preferably select the seismic data records from networks with relatively small apertures. The coherent pmP arrivals shown in each section and the vespagrams ensure that the crustal thickness remains nearly constant over an area defined by the event-network distributions; this makes linearly stacking the waveforms feasible.

3.2. Estimation of Vp in the crust

In reality, the crustal material is not homogeneous but laminated, and is conventionally divided into two layers consisting of the more felsic upper crust and the more mafic lower crust. P waves propagate in different layers with different velocities. Therefore, we used the averaged crustal velocity of P waves in the study region to derive the crustal thickness.

Pn and its depth phases (i.e., pPn and sPn) have been used to constrain the average crustal velocity and focal depth; however, this approach requires accurate depth-phase identification (e.g., Stroujkova, 2009). Pg arrival times collected from the ISC bulletin have been used to yield a crustal velocity of 6.20 km/s in the Central Andes (McGlashan et al., 2008). Here, we manually picked the arrival-times of Pg to constrain the average crustal velocity.

To ensure that the constrained velocity represents the entire crust rather than the upper layer or the lower crust/uppermost mantle, the selected epicentral distance was strictly constrained between 0.5 and 2.5°. In addition, the selected earthquakes occurred at depths of 19.5–56.2 km to ensure that the entire crust could be adequately sampled by variously sourced Pg waves. Finally, a total of 25 Pg arrivals were manually picked to estimate the average crustal velocity (Fig. 4). We plotted the 25 arrival-times versus the hypocenter-station distance (i.e., considering the focal depth effect) rather than the epicentral distance, so that the fitting velocity would be very close to the average velocity. Our careful analyses yielded an approximate estimate of the velocity of ~6.21 km/s with a deviation of 0.22 km/s in the crust. This value is similar to the velocity derived in the Central Andes of 6.20 km/s (McGlashan et al., 2008) and the velocity used in receiver function studies in Pamir (Schneider, 2014); in addition, it falls into the range of the average crustal velocity for global orogens of 6.39 km/s with a standard deviation of 0.25 km/s (Christensen and Mooney, 1995). If we assume that the uncertainty of the event depths can be up to 10 km, the resulting deviation in the fitted velocity would be <0.10 km/s based on a standard IASP91 model, which is acceptable when estimating the crustal thickness.

4. Results and discussion

4.1. Crustal thickness variations of this region

Using the average velocity of the P wave (~6.21 km/s) in the crust, we obtained a total of four estimates varying from 58.1 km to 76.2 km. Note that the derived P wave velocity was only applied to the four estimates, whereas the deep double reflection interfaces were inferred by waveform modeling via trial and error because a more complicated structure was required. Fig. 5 displays the measured crustal thickness with spatially varying deviations in the intermediate-depth seismic zone (36–37°N, 69–72°E). This result may indicate that the Moho structure beneath the Pamir–Hindu Kush is very complicated and exhibits strong lateral variations. From the distribution of the four estimates (Fig. 5), we can see that northwest of the three events, the crust gradually thickens eastward, which is associated with the subduction of the Indian Plate. Northeast of the events, the crustal thickness abruptly increases southward, which may be associated with the subduction of the Eurasian Plate.

The thinnest crust of 58.1 km occurs in the eastern margin of the Tadjik Basin, reflecting that this stable block has suffered less collisional deformation, while the double reflections down to ~97 km take place in the junction of the Indian and Eurasian Plates, where the Eurasian Plate subducted beneath the Pamir, mirroring the remarkable thickening history of collisional plates. We propose a scenario to explain the deepest observed signature in the later sub-section.

4.2. Depth section in the north-south direction

To better understand the geometry of Moho structures, event distributions, and interactions between the Indian and Asia Plates in the study area, a schematic north-south cross section was constructed (Fig. 6). The event catalogue was taken from the relocation results given by Sippl et al. (2013a). Our three selected events occurred at intermediate depths. The sub-Moho events appear to cluster in the upper layer of the subducted plate, which was interpreted as being the lower crust of the Indian Plate (e.g., Kufner et al., 2016). Slab break-off resulting from possible tearing has been used to explain the cause of the terminal stage of subduction beneath the Hindu Kush (e.g., Kufner et al., 2017). To the west of this profile, the crust thickens southward from 59 km to 66 km, perhaps as a result of the Eurasian Plate subduction beneath the Pamir, as seen from receive function (Schneider et al., 2013).

4.3. Depth section in the west-east direction

The results from receiver function studies (e.g., Schneider et al., 2013) were selectively incorporated into the W-E oriented cross section BB' (Fig. 7). We can clearly see that the depth of the reflection interface increases from west to east with depths varying from 44 km beneath the Tadjik basin to ~97 km beneath the southernmost Pamir. In the central Tadjik Basin, previous studies have derived a crustal thickness of approximately 45 km based on receiver functions calculated at three stations (Schneider et al., 2013). The crust thickens to 58 km eastward and reaches 76 km at the easternmost margin, which is believed to result from the Indian Plate's northward indention. The estimate of 76 km is located close to the Darvaz transform fault (Sippl et al., 2013a), where the Tajik Basin terminates to the east. Note that the source-sided approach to determining the crustal thickness avoids the contamination of multiples in the sediments of basins, whereas approaches using receiver functions are often complicated due to

Please cite this article as: He, H., et al., Subducting continental lower crust and crustal thickness variations in the intermediate seismic zone of Pamir–Hindu Kush inferre..., Tectonophysics (2017), http://dx.doi.org/10.1016/j.tecto.2017.04.004

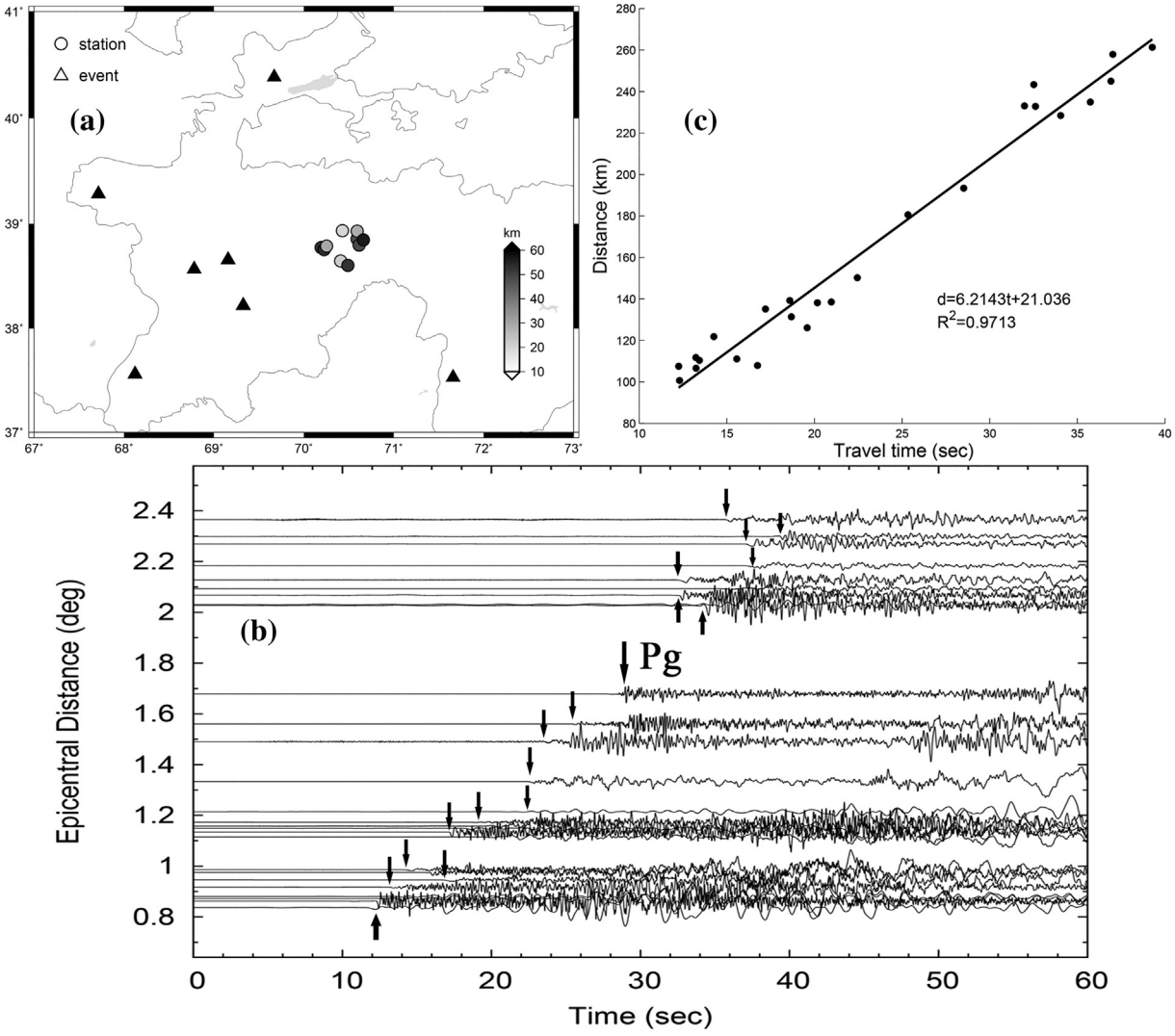

Fig. 4. (a) Distribution of 10 events and 7 stations selected for Pg measurements. (b) 25 traces from various events are arranged to produce a section, and the Pg onset is manually marked by arrows. (c) Plot of Pg traveltime versus hypocenter-station propagation distance. The slope of this plot yields a crude estimate of average crustal velocity (6.21 km/s) with a deviation of 0.22 km/s via linear regression analysis.

interference from strong reverberations in the sediments for stations located in basins (Zheng et al., 2005).

The deepest interface is detected at the junction where the Indian and Eurasian Plates meet at depth beneath the northernmost Hindu Kush. We can clearly see that the crustal thickening to 76 km results from the subduction of the Indian Plate beneath the Hindu Kush. Our observations complement the receiver function results and offer a better understanding of the evolution of the Tajik Basin and it surroundings in response to its contact with the northward moving Indian Plate. Conversely, the double reflection is suspected of being a consequence of the subduction of the Eurasian Plate beneath the southernmost Pamir, which can be seen more readily in the CC' profile (Fig. 8b) in the next sub-section.

4.4. Seismic signature of the deeply subducted Eurasian lower crust

In addition to having obtained several estimates of the crustal thickness over various locations, the most interesting and striking signature in this study was the detection of double reflection arrivals beneath the southernmost Pamir, which is as deep as ~97 km; these detections may help describe the deep structure in this region, even though it is a challenge to explain it based on one event record-section alone (Fig. 8a).

Fig. 8(a) displays a record-section from F-net recording an event that occurred on December 12, 2015, comprised of two pronounced arrivals with opposite polarities (highlighted by the red and blue shadows) between P and pP. We can readily understand that the polarity change is due to a variation in the seismic impedance contrast across the deep interfaces. Previous seismic investigations have suggested that the continental Eurasian lower crust has been subducting beneath the Pamir based on receiver function analyses (Schneider et al., 2013) and local earthquake tomography (Sippl et al., 2013b). Even though their data are primarily located north of Pamir, we constructed a similar model to conduct waveform simulations in the southernmost Pamir (Fig. 8c).

From the geometric configuration of the subducted lower crust, we expect to see a change of polarity occur when incoming waves meet different interfaces that separate the lower crust from the ambient mantle. The resulting polarities are marked by plus and minus signs. In addition, we also interpret the lack of strong second reflection arrivals in the top two traces and the first arrivals in the lowest three traces in the record section to be due to (1) the small impedance contrast that occurs in the interface of the lower Eurasian lower crust overlying the Indian lower crust, whereas a large contrast is generated at the contact with the ambient mantle, and (2) defocusing that occurs when an incoming wave meets a curved interface. The upper interface of the Eurasian

Please cite this article as: He, H., et al., Subducting continental lower crust and crustal thickness variations in the intermediate seismic zone of Pamir–Hindu Kush inferre..., Tectonophysics (2017), http://dx.doi.org/10.1016/j.tecto.2017.04.004

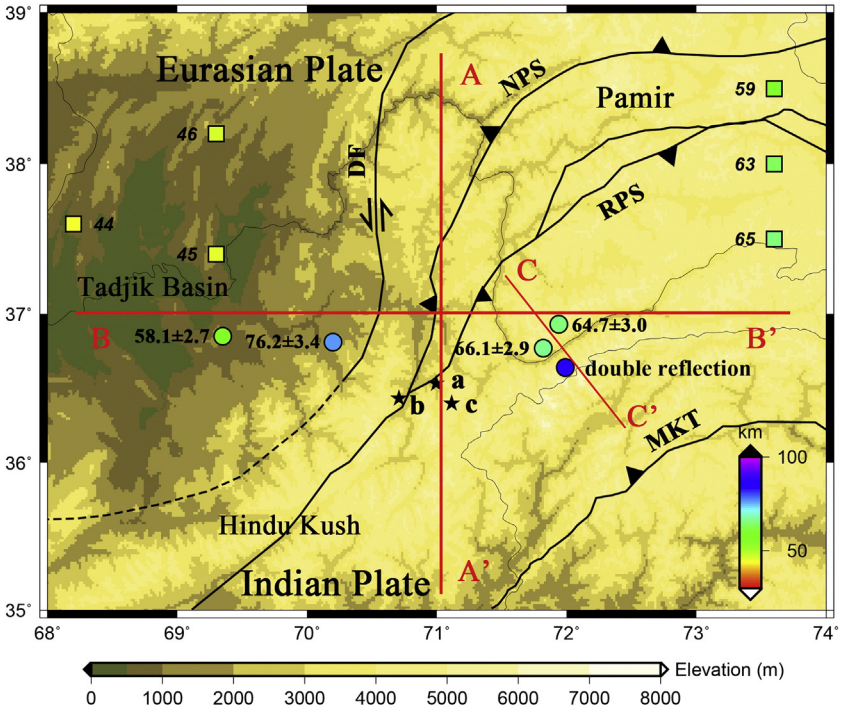

Fig. 5. Map showing the location of the three events used (black stars), crustal thickness variations along with calculated uncertainties from this study (colored circles), and selected thickness values in adjacent areas derived from receiver function studies by Schneider (2014) (colored squares). The blue solid circle denotes the locus where a double reflection occurs from two deep interfaces at ~97 km. The locations of cross-sections (AA', BB', and CC') are depicted by red lines. (For interpretation of the references to color in this figure legend, the reader is referred to the web version of this article.)

lower crust is less curved where reflections occur likely due to tight contact with the overlying Indian crust.

To take the lateral structural variations into account in a complex geologic environment, two 1D models were constructed by trial and error. The velocity models used to do the simulations are presented in Fig. 8b2 and b3. Below 120 km, the IASP91 model is incorporated. Our modeling explains both the negative and positive arrivals surprisingly well in terms of the arrival time, relative amplitude, and polarity (Fig. 8b1). From the two velocity depth profiles, we can see that the first double reflection occurs at ~72 km and ~95 km, vertically spaced by 23 km, whereas the second deeper double reflection occurs at ~86 km and ~97 km, vertically spaced by 11 km. Our analysis implies that the subducted lower part of crust has gradually thinned with increasing depth. Receiver functions have revealed that a low-velocity layer related to the subducted lower continental crust has a 10–15 km thickness at large depths (Schneider et al., 2013), which is consistent with our findings. The deep interface detected here coincides with the deepest focal depth of ~90 km for events occurring in this area (Sippl et al., 2013a). This coincidence likely reflects that the intermediate-depth events preferably take place in the subducted lower crust due to metamorphic dehydration reactions (Sippl et al., 2013b).

To better understand the lateral variations in the polarities and deep structures, a map is presented in Fig. 8 in order to illustrate the estimates from our double reflections along with two previous thickness estimates of 65 km and 66 km thickness, which are spatially close to the two double reflection locations. The underside-reflection sites from the two vertically spaced interfaces are denoted in two colored solid circles, the upper interface in blue and the lower interface in red (dashed when weak or invisible in the data section). We can clearly

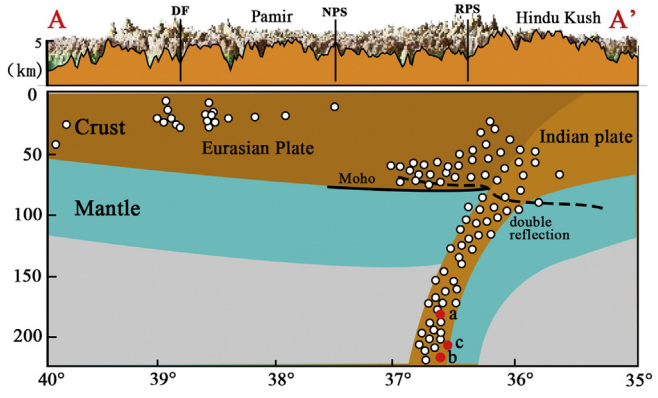

Fig. 6. Cross-section along 71°E (AA') schematically illustrating the hypocenters of 3 selected events (red dots) located in the subducted Indian plate along with locations of major earthquakes (black dots) which occurred in this slice provided by Sippl et al. (2013a). Black lines (dashed when not in the same section plane, but projected) denote the possible Moho interfaces of the Indian and Asian Plates. (For interpretation of the references to color in this figure legend, the reader is referred to the web version of this article.)

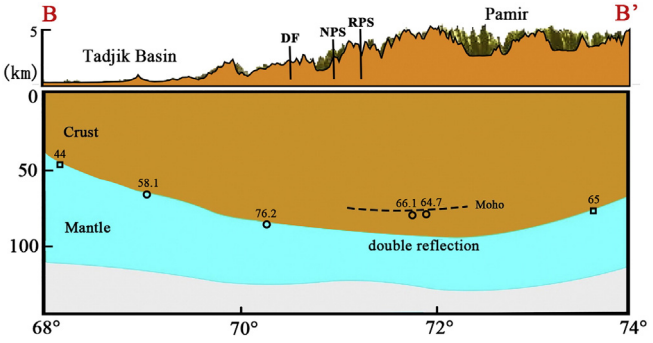

Fig. 7. Cross-section along 37°N (BB') schematically illustrates Moho undulation inferred from measured crustal thicknesses in this study (circles) with selected receiver function results (squares). Note that the measurements (such as the estimates on the dashed line), which are not exactly located along this profile, are also plotted to roughly demonstrate Moho undulation.

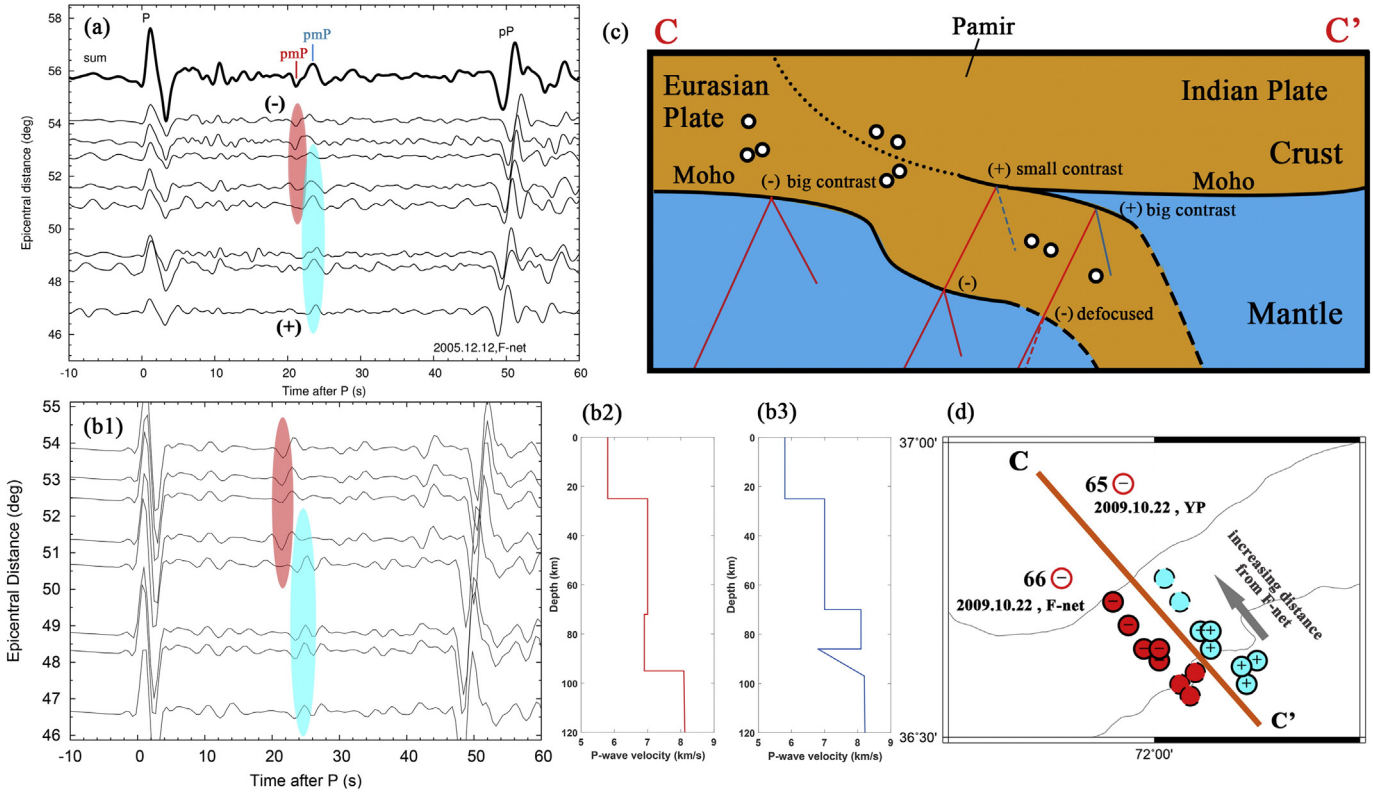

Fig. 8. (a) The record-section for the event on 2005 December 12 recorded by F-net showing P, pmP, and pP; two reflected arrivals are detected with different polarity highlighted by colored ellipses. (b1) The calculated synthetic section according to the models plotted in b2 and b3 which reproduce the two reflections. (c) A sketch presenting the cross-section CC' to display the configuration of subducted Asian lower crust structure along with the foci of major events which occurred in this slice taken from the relocation catalogue given by Sippl et al. (2013a). Positive impedance contrasts relative to pP are marked with a plus sign; negative values are marked with a minus sign. The red lines denote ray-paths of underside reflected P waves, and incoming wave becomes defocused when reflected from a strongly curved interface. (d) The spatial distribution of under-side reflected points from two deep interfaces spaced vertically by 15 km depicted in solid blue and red circles (dashed when weak or invisible in record section) along with each arrival's polarity sign. Two other estimates along with their polarities are also presented for comparison. (For interpretation of the references to color in this figure legend, the reader is referred to the web version of this article.)

see a southeastward thickening trend from 65 to 66 km to the two upper interfaces of ~72–86 km.

Note that small variations may exist in the derived interface depths among the different reflections based on each trace; however, we only considered two simplified uniform models. Our forward modeling not only successfully reproduces the dominant phases of P, pP, and pmP, but also excellently simulates two prominent secondary phases (Fig. 8b1). The first is ~10 s after the P wave, and the second is ~5 s before the pP wave. According to our constructed models, both are likely relevant to a crustal interface. The first is a multiple wave that occurs between the free surface and the interface below the stations, while the second is an under-side reflection from the interface above the sources.

An estimate of the crustal shortening budget during the Indian-Eurasian convergence indicates that a significant amount of continental crust must have been lost, most likely having been recycled into the mantle (Schmidt et al., 2011); this is consistent with our observations. In addition, eclogite, an indicator of the occurrence of high-pressure metamorphism (Bascou et al., 2001), has been identified in this region (e.g., O'Brien et al., 2001; Hacker et al., 2005), implying that crustal rocks have resided at depths > ~90 km beneath the Pamir, which supports our observations.

4.5. Limitations and measurement uncertainties

Even though we obtained four reliable estimates of the crustal thickness, their spatial distribution was still limited, mostly due to the small number of moderate to large events from intermediate depths; such large events primarily occurred in the subducted Indian Plate, whereas those occurring in the subducted Eurasian Plate were relatively small (Pegler and Das, 2002; Sippl et al., 2013a; Bai and Zhang, 2015).

The uncertainty in the estimates of the crustal thickness mostly arises from the V_{pc} measurement, whereas the uncertainty in V_{pc} is primarily caused by the deviation in the focal-depths and insufficient Pg arrivals to adequately sample the crust. As we estimated in the previous section, a 10 km uncertainty in the event depths only produces a deviation in V_{pc} of <0.10 km/s, which is acceptable to constrain the crustal thickness. Even though the deviation in V_{pc} can be up to 0.22 km/s, as our regression demonstrated, the resulting uncertainty in the crustal thickness is <3 km. Moreover, our efforts in careful selecting data resulted in a large number of Pg arrivals, which ensured that the crust was adequately sampled through the upper and lower layers. However, it is noteworthy that the event-station pairs for the Pg collection are distributed centrally in Pamir (Fig. 4), and rarely in Hindu Kush, which may introduce a bias for some measurements of the Hindu Kush considering the strong lateral velocity variations in such a complex tectonic unit.

5. Conclusion

The Pamir-Hindu Kush to the northwest of Tibet plateau is part of an active continental collision, which has produced a sizeable region of thickened continental crust. There is, however, no general agreement on the mechanisms of the crustal thickening, partly because the crustal thickness of the Pamir-Hindu Kush still remains poorly determined. In this study, we analysed phases from three intermediate-depth earthquakes comprising P, pmP, and pP waves which were collected from F-net and IRIS, to constrain the crustal thickness in the seismic zone of the Pamir-Hindu Kush region. We obtained four estimates at different

Please cite this article as: He, H., et al., Subducting continental lower crust and crustal thickness variations in the intermediate seismic zone of Pamir–Hindu Kush inferre..., Tectonophysics (2017), http://dx.doi.org/10.1016/j.tecto.2017.04.004

locations, which vary between 58 km to 76 km. These results represent important constraints for any future geodynamic modeling of this collision zone. We explain that the deepest interface at a depth of ~97 km beneath the southernmost Pamir likely reflects the presence of the subducted Eurasian lower crust in the study area. Our observations complement those provided by previous studies (e.g., receiver function analysis) undertaken in this region.

Acknowledgements

The authors acknowledge the F-net and the IRIS consortia for the availability of the waveform data for this study. We thank Prof. Nick Rawlinson (guest editor) and Dr. Ramon Carbonell (editor) along with Dr. Simone Pilia and two anonymous reviewers for careful and constructive review comment. Figures were made with GMT (Wessel and Smith, 1995) and GNUPLOT. This work was supported by the National Science Foundation of China (Grant No. 41330207).

Appendix A. Supplementary data

Supplementary data to this article can be found online at http://dx.doi.org/10.1016/j.tecto.2017.04.004.

References

Bai, L., Zhang, T., 2015. Complex deformation pattern of the Pamir-Hindu Kush region inferred from multi-scale double-difference earthquake relocations. Tectonophysics 638, 177–184.

Bascou, J., Barruol, G., Vauchez, A., Mainprice, D., Egydiosilva, M., 2001. EBSD-measured lattice-preferred orientations and seismic properties of eclogites. Tectonophysics 342 (1), 61–80.

Burtman, V.S., Molnar, P., 1993. Geological and geophysical evidence for deep subduction of continental crust beneath the Pamir. Spec. Pap. Geol. Soc. Am. 281 (2), 248–251.

Christensen, N.I., Mooney, W.D., 1995. Seismic velocity structure and composition of the continental crust: a global view. J. Geophys. Res. 100 (B7), 9761–9788.

Crotwell, H.P., Owens, T.J., Ritsema, J., 1999. The TauP toolkit: flexible seismic travel-time and ray-path utilities. Seismol. Res. Lett. 70, 154–160.

Feng, B., Pei, S., 2012. Pn wave velocity and anisotropy beneath Pamir and its adjacent regions. Earthq. Sci. 25, 485–493.

Hacker, B., Luffi, P., Lutkov, V., Minaev, V., Ratschbacher, L., Plank, T., Ducer, M., P.-Douce, A., McWillims, M., Metcalf, J., 2005. Near-ultrahigh pressure processing of continental crust: miocene crustal xenoliths from the Pamir. J. Petrol. 46 (8), 1661–1687.

Kennett, B.L.N., Engdahl, E.R., 1991. Travel times for global earthquake location and phase identification. Geophys. J. Int. 105, 429–465.

Kufner, S.K., Schurr, B., Sippl, C., Yuan, X., Ratschbacher, L., Akbar, A.S.M., et al., 2016. Deep India meets deep Asia: lithospheric indentation, delamination and break-off under Pamir and Hindu Kush (Central Asia). Earth Planet. Sci. Lett. 435, 171–184.

Kufner, S.K., Schurr, B., Haberland, C., Zhang, Y., Saul, J., Ischuk, A., Oimahmadov, I., 2017. Zooming into the Hindu Kush slab break-off: a rare glimpse on the terminal stage of subduction. Earth Planet. Sci. Lett. 461, 127–140.

McGlashan, N., Brown, L., Kay, S., 2008. Crustal thickness in the central Andes from teleseismically recorded depth phase precursors. Geophys. J. Int. 175 (3), 1013–1022.

Mechie, J., Yuan, X., Schurr, B., Schneider, F., Sippl, C., Ratschbacher, L., Minaev, V., Gadoev, M., Oimahmadov, I., Abdybachaev, U., Moldobekov, B., Orunbaev, S., Neg- Matullaev, S., 2012. Crustal and uppermost mantle velocity structure along a profile across the Pamir and southern Tien Shan as derived from project TIPAGE wide-angle seismic data. Geophys. J. Int. 188, 385–407.

Negredo, A.M., Replumaz, A., Villaseñor, A., Guillot, S., 2007. Modeling the evolution of continental subduction processes in the Pamir–Hindu Kush region. Earth Planet. Sci. Lett. 259 (1), 212–225.

O'Brien, P.J., Zotov, N., Law, R., Khan, M.A., Jan, M.Q., 2001. Coesite in Himalayan eclogite and implications for models of India-Asia collision. Geology 29 (5), 435–438.

Patriat, P., Achache, J., 1984. India-Eurasia collision chronology has implications for crustal shortening and driving mechanism of plates. Nature 48 (2), 615–621.

Pegler, G., Das, S., 2002. An enhanced image of the Pamir-Hindu Kush seismic zone from relocated earthquake hypocentres. Geophys. J. Int. 134 (2), 573–595.

Robinson, A., Yin, A., Manning, C., Harrison, T.M., Zhang, S.H., Wang, X.F., 2004. Tectonic evolution of the northeastern Pamir: constraints from the northern portion of the Cenozoic Kongur Shan extensional system, western China. Geol. Soc. Am. Bull. 116, 953–973.

Schmidt, J., Hacker, B.R., Ratschbacher, L., Stubner, K., Stearns, M., K.-Clark, A., Cottle, J.M., Webb, A.A.G., Gehrels, G., Minaev, V., 2011. Cenozoic deep crust in the Pamir. Earth Planet. Sci. Lett. 312, 411–421.

Schneider, F.M., Yuan, X., Schurr, B., Mechie, J., Sippl, C., Haberland, C., Minaev, V., Oimahmadov, I., Gadoev, M., Radjabov, N., Abdybachaev, U., Orunbaev, S., Negmatullaev, S., 2013. Seismic imaging of subducting continental lower crust beneath the Pamir. Earth Planet. Sci. Lett. 375 (8), 101–112.

Schneider, F.M., 2014. Imaging an Intra-continental Subduction in Central Asia With Teleseismic Receiver Functions. (PhD Thesis Potsdam: Deutsches GeoForschungsZentrum GFZ). http://dx.doi.org/10.2312/GFZ.b103-14063.

Schwab, M., Ratschbacher, L., Siebel, W., Mcwilliams, M., Minaev, V., Lutkov, V., et al., 2004. Assembly of the Pamirs: age and origin of magmatic belts from the southern tien shan to the southern Pamirs and their relation to Tibet. Tectonics 23 (4), 443–459.

Sippl, C., Schurr, B., Yuan, X., Mechie, J., Schneider, F.M., Gadoev, M., et al., 2013a. Geometry of the Pamir-Hindu Kush intermediate-depth earthquake zone from local seismic data. J. Geophys. Res. Solid Earth 118 (4), 1438–1457.

Sippl, C., Schurr, B., Tympel, J., Angiboust, S., Mechie, J., Yuan, X., Schneider, F.M., Sobolev, S.V., Ratschbacher, L., Haberland, C., TIPAGE-Team, 2013b. Deep burial of Asian continental crust beneath the Pamir imaged with local earthquake tomography. Earth Planet. Sci. Lett. 384, 165–177.

Sobel, E.R., Chen, J., Schoenbohm, L.M., Thiede, R., Stockli, D.F., Sudo, M., et al., 2013. Oceanic-style subduction controls late Cenozoic deformation of the northern Pamir orogen. Earth Planet. Sci. Lett. 363 (2), 204–218.

Stroujkova, A., 2009. Constraining event depths and crustal velocities using regional depth phases. Bull. Seismol. Soc. Am. 99 (1), 215–225.

Wang, R., 1999. A simple orthonormalization method for stable and efficient computation of Green's functions. Bull. Seismol. Soc. Am. 89, 733–741.

Wessel, P., Smith, W.H.F., 1995. New version of the generic mapping tools. EOS Trans. Am. Geophys. Union 76 (33):329. http://dx.doi.org/10.1029/95EO00198.

Yang, Z., He, X., 2015. Oceanic crust in the mid-mantle beneath West-Central Pacific subduction zones: evidence from S to P converted waveforms. Geophys. J. Int. 203 (1):541–547. http://dx.doi.org/10.1093/gji/ggv314.

Zandt, G., Velasco, A.A., Beck, S.L., 1994. Composition and thickness of the southern altiplano crust, Bolivia. Geology 22 (11), 1003–1006.

Zhang, Z., Lay, T., 1993. Investigation of upper mantle discontinuities near northwestern pacific subduction zones using precursors to sSH. J. Geophys. Res. Solid Earth 98 (B3), 4389–4405.

Zheng, T., Zhao, L., Chen, L., 2005. A detailed receiver function image of the sedimentary structure in the Bohai Bay basin. Phys. Earth Planet. Inter. 152, 129–143.

Please cite this article as: He, H., et al., Subducting continental lower crust and crustal thickness variations in the intermediate seismic zone of Pamir–Hindu Kush inferre..., Tectonophysics (2017), http://dx.doi.org/10.1016/j.tecto.2017.04.004